Research Article | Vol. 26, No. 20 | 1 Oct 2018 | OPTICS EXPRESS 26020
Optics EXPRESS

Determination of the thermally induced focal shift of processing optics for ultrafast lasers with average powers of up to 525 W

SEBASTIAN FAAS,* DANIEL J. FOERSTER, RUDOLF WEBER, AND THOMAS GRAF

Institut für Strahlwerkzeuge IFSW, Pfaffenwaldring 43, 70569 Stuttgart, Germany
**sebastian.faas@ifsw.uni-stuttgart.de*

Abstract: The continuous increase of the average laser power of ultrafast lasers is a challenge with respect to the thermal load of the processing optics. The power which is absorbed in an optical element leads to a temperature increase, temperature gradients, changing refractive index and shape, and finally causes distortions of the transmitted beam. In a first-order approximation this results in a change of the focal position, which may lead to an uncontrolled change of the laser machining process. The present study reports on investigations on the focal shift induced in thin plano-convex lenses by a high-power ultra-short pulsed laser with an average laser power of up to 525 W. The focal shift was determined for lenses made of different materials (N-BK7, fused silica) and with different coatings (un-coated, broadband coating, specific wavelength coating).

1. Introduction

To focus a laser beam, e.g. onto the surface of the workpiece, mainly transmissive laser optics are used which are transparent at the wavelength of the laser beam. Still, a small amount of laser energy is absorbed within the transmissive optics and the coatings on their surfaces. Contaminations on the surface and imperfections within the substrate can augment this effect. When using high-power laser beams, the local absorption in the optics can lead to strong temperature gradients. Due to the temperature dependence of the refractive index [1,2] this induces gradients of the refractive index perpendicular to the propagation axis of the laser beam, resulting in distortions of the phase front. In a first-order approximation the distortions are spherical and can be described by a thermally induced lens with the corresponding shift of the focal position. The phase-shift is caused by the temperature gradients in the optics and cannot be avoided with cooling of the optics [3]. The higher-order, i.e. non-spherical distortions deteriorate the beam quality and hence result in an increased value of the beam propagation factor M^2. In the following we concentrate on the thermally induced focal shift since it is the most relevant disturbance that needs to be taken into account when designing laser machining processes.

In the field of laser precision machining, e.g. surface ablation and drilling, the physical processes first of all depend on the incident fluence $H = E_P / A$, where E_P is the energy of the laser pulse and $A = \frac{1}{4} \cdot \pi \cdot d_b^2$ is the irradiated area given by the diameter d_b of the beam on the workpiece. Processing in the focal plane of the focusing optics is the most common approach, since the highest fluence can be achieved at this position. When the position of the beam waist shifts by one Rayleigh length due to thermally induced effects, the fluence on the workpiece at the original position of the nominal focal plane decreases by a factor of 2 [4]. As the applied fluence significantly influences the efficiency of e.g. surface ablation [5], the thermally induced focal shift can dramatically reduce the processing efficacy. When working close to the ablation threshold, as in the case of surface structuring [6], the ablation process can stop completely even for small changes of the focal position. During laser drilling, the

#340915 https://doi.org/10.1364/OE.26.026020
Journal © 2018 Received 30 Jul 2018; revised 9 Sep 2018; accepted 9 Sep 2018; published 20 Sep 2018

Optics EXPRESS

shift of the focal position results in less pulse energy coupled into the hole due to the enlarged beam diameter at the position of the workpiece. Alternatively, this may lead to an unwanted widening of the inlet of the hole. Within the hole, a reduced available fluence can lead to the formation of thermal damage due to heat accumulation [7–9].

In previous studies the effects of the thermally induced focal shift in focusing optics was investigated experimentally for continuous wave lasers in the field of macro materials processing, e.g. by using the threshold of deep-penetration welding [10]. For precision machining ultrashort-pulsed (USP) lasers are commonly used. USP lasers with an average laser power of more than 1 kW are already available for laboratory use [11] and the average laser power of USP lasers is growing steadily [12,13]. With the increasing average power of the USP lasers the thermally induced focal shift in the laser optics now becomes so large also in the field of micro materials processing that it can no longer be neglected. In the present study we determine the thermally induced refractive power caused by the average laser power of thin plano-convex lenses that are typically used for micro materials processing with USP lasers. The thermally induced lens, which is responsible for the thermally induced focal shift, was directly determined by measuring the beam caustic around the focal plane for different average laser powers.

2. Thermally induced focal shift of a single lens

The refractive power $1/f_{tot}$ of a focusing lens including the contribution $1/f_{th}$ of the thermally induced lens, where f_{tot} and f_{th} are the corresponding focal lengths, can be expressed by [14,15]

$$\frac{1}{f_{tot}} = \frac{1}{f_0} + \frac{1}{f_{th}} = \frac{1}{f_0} + \frac{D^* \cdot P_i}{\pi \cdot w_i^2} = \frac{1}{f_0} + D^* \cdot I_i = \frac{1 + f_0 \cdot D^* \cdot I_i}{f_0}, \tag{1}$$

where $1/f_0$ is the refractive power of the cold unperturbed lens, D^* is the intensity-specific thermal refractive power of the lens, w_i is the beam radius incident on the optics, P_i is the average power incident on the optics, and $I_i = P_i / (\pi \cdot w_i^2)$ is the intensity incident on the focusing lens. To assess the influence of the thermally induced lens it is convenient to relate the thermally induced focal shift $\Delta f = f_{tot} - f_0$ to the Rayleigh length z_R. Using Eq. (1) this leads to

$$\frac{\Delta f}{z_R} = \frac{f_{tot} - f_0}{z_R} = \frac{1}{z_R} \cdot \left(\frac{f_0}{1 + f_0 \cdot D^* \cdot I_i} - f_0 \right) = - \frac{f_0^2 \cdot D^* \cdot I_i}{z_R \cdot \left(1 + f_0 \cdot D^* \cdot I_i\right)}. \tag{2}$$

When the thermally induced refractive power is much smaller than the refractive power of the unperturbed lens, i.e. $1/f_{th} \ll 1/f_0$, which is equivalent to $\pi \cdot w_i^2 / (D^* \cdot P_i) \gg f_0$ and hence $1 \gg f_0 \cdot D^* \cdot I_i$, Eq. (2) can be approximated by

$$\frac{\Delta f}{z_R} \cong - \frac{f_0^2 \cdot D^* \cdot I_i}{z_R} = - \frac{f_0^2 \cdot D^* \cdot P_i}{z_R \cdot \pi \cdot w_i^2}. \tag{3}$$

With the known relations for the radius of the waist of the focused beam [16]

$$w_0 = - \frac{f_0 \cdot \lambda \cdot M^2}{\pi \cdot w_i} \tag{4}$$

and the Rayleigh length [16]

Optics EXPRESS

$$z_R = -\frac{\pi \cdot w_0^2}{\lambda \cdot M^2}, \tag{5}$$

where λ is the wavelength of the laser beam and M^2 is the beam propagation factor, Eq. (3) can be rewritten as

$$\frac{\Delta f}{z_R} \cong -\frac{D^*}{\lambda \cdot M^2} \cdot P_i \tag{6}$$

which is a simplified expression for the power-dependent thermally induced focal shift.

3. Experimental investigations

To determine the thermally induced shift of the focal position caused by high average laser powers transmitted through a thin lens, a home-built ultrafast laser (wavelength λ = 1030 nm, pulse duration 8 ps, pulse repetition rate f = 300 kHz, currently with an average power of up to P = 525 W) was used [12]. The laser beam was linear polarized. All experiments were performed at a room temperature of 22 °C and a humidity of 60%.

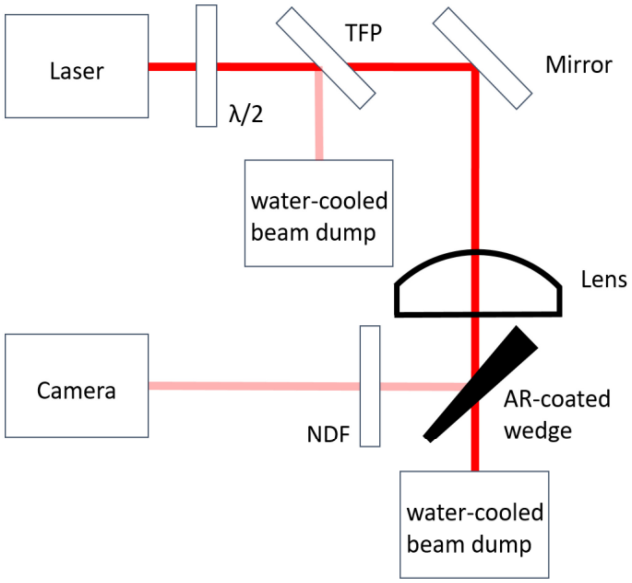

Fig. 1. Experimental setup for the measurement of the thermally induced shift of the focal position of thin lenses. A neutral-density filter (NDF) attenuates the beam reflected by the AR-coated wedge to avoid damages of the CCD chip of the camera.

The experimental setup is shown in Fig. 1. The average laser power incident on the focusing thin lens was controlled by a combination of a half-wave plate (λ/2) and a thin-film polarizer (TFP). The reflected beam was absorbed by a water-cooled beam dump. The radius of the collimated beam incident on the focusing optics was w_{cb} = 2.5 mm and the intensity distribution was Gaussian. The lens under test was used to focus the laser beam propagating towards an AR-coated wedge, which was used as a beam splitter. The transmitted beam was absorbed by a water-cooled beam dump. The reflected beam was analyzed by a CCD camera and was therefore attenuated by a reflective neutral-density filter (NDF) to avoid damages of the CCD chip. The distance d between the focusing optics and the NDF was always 65 mm. Although a reflective NDF was used, this cannot completely avoid thermally induced lensing also by the filter. In order to exactly identify the thermally induced focal shift of the tested focusing lens the influence of the NDF has therefore to be known and taken into account. The

Optics EXPRESS

influence of thermally induced focal shift occurring in the NDF and its separation from the focal shift induced in the tested lens is discussed in the Appendix.

Table 1 lists the specifications of all investigated lenses. Lenses provided by different companies and with different focal lengths were used in this study. Different lenses made of either fused silica (FS) or N-BK7 and with either a broadband coating (BBC), a specific wavelength coating (WLC), or uncoated (UC) lenses were compared. N-BK7 lenses were investigated since they are interesting for low-power applications and to serve as a reference for the capabilities of the fused silica lenses at high average laser powers. Additionally, the condition of each lens is listed since we also compared new lenses to lenses that have been used before in other experiments.

3.1 The measured total thermally induced focal shift

The total thermally induced focal shift Δf_{tot} measured by the experimental setup described above comprises the contributions from both the lens under test and the NDF. As derived in the Appendix (Eq. (12)) this combined effect is expressed by

$$\frac{\Delta f_{tot}}{z_R} \cong -\frac{f_0^2 \cdot D^* \cdot I_i + f_0^2 \cdot D^*_{NDF} \cdot \frac{R \cdot I_i}{1 - d/f_0} - d \cdot f_0 \cdot D^*_{NDF} \cdot \frac{R \cdot I_i}{1 - d/f_0} - d \cdot f_0^2 \cdot D^* \cdot I_i \cdot D^*_{NDF} \cdot \frac{R \cdot I_i}{1 - d/f_0}}{z_R \cdot \left(1 + f_0 \cdot D^*_{NDF} \cdot \frac{R \cdot I_i}{1 - d/f_0} - d \cdot D^*_{NDF} \cdot \frac{R \cdot I_i}{1 - d/f_0}\right)}. \quad (7)$$

where D^*_{NDF} is the intensity-specific thermal refractive power of the NDF, and R is the reflectivity of the beam splitter. Hence, in order to extract the sole contribution of the tested lens, we first needed to determine the specific thermal refractive power D^*_{NDF} of the NDF. The procedure is described in the Appendix and resulted in the value of $D^*_{NDF} = 3.32 \cdot 10^{-4}\ mm/W$.

Note that since the location of the beam waist cannot be measured without a beam of finite power, the reference with $I_i = 0$ and $\Delta f_{tot} = 0$ is usually not well defined in the experiment. Instead, the determination of Δf_{tot} as a function of the applied intensity I_i may first be measured with respect to an arbitrary reference with an initially unknown offset Δf_0. Equation (7) therefore is changed to

$$\frac{\Delta f_{tot}}{z_R} \cong -\frac{f_0^2 \cdot D^* \cdot I_i + f_0^2 \cdot D^*_{NDF} \cdot \frac{R \cdot I_i}{1 - d/f_0} - d \cdot f_0 \cdot D^*_{NDF} \cdot \frac{R \cdot I_i}{1 - d/f_0} - d \cdot f_0^2 \cdot D^* \cdot I_i \cdot D^*_{NDF} \cdot \frac{R \cdot I_i}{1 - d/f_0}}{z_R \cdot \left(1 + f_0 \cdot D^*_{NDF} \cdot \frac{R \cdot I_i}{1 - d/f_0} - d \cdot D^*_{NDF} \cdot \frac{R \cdot I_i}{1 - d/f_0}\right)} + \Delta f_0, \quad (8)$$

With this and the known contribution of the NDF the thermal refractive power D^* of the lens under test can be extracted by fitting Eq. (8) to the measured values of Δf_{tot} and using D^* and Δf_0 as the fitting parameters. For the example of the tested lens no. 2 (see Table 1) this is shown by Fig. 2. The error bars shown in the figure indicate the uncertainty associated with the experimental determination of the focal position and was estimated to be approximately one quarter of z_R.

Optics EXPRESS

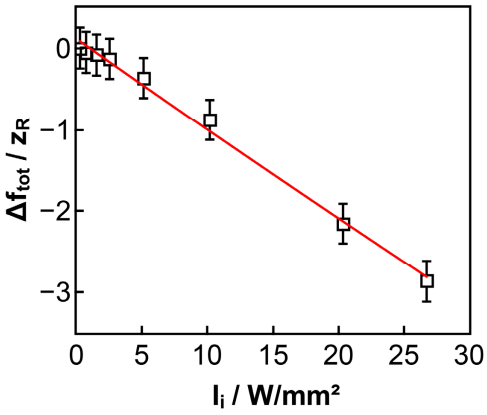

Fig. 2. Measured thermally induced total focal shift with lens no. 2 in the testing setup (square points). The red curve is given by Eq. (8) which was fitted to the measured data. The least-square fit led to $D^* = 0.77 \cdot 10^{-6}$ mm/W . Laser parameters: λ = 1030 nm, M^2 = 1.2, f = 300 kHz.

3.2 Thermal refractive power of thin lenses

Table 1 lists the thermal refractive power of all tested lenses which was determined by a least-square fit of Eq. (8) to the measured intensity-dependent total focal shift Δf_{tot} as described above.

The measurements with the uncoated lenses 5, 6, and 9 yield the thermal refractive power caused by the sole substrate, including the potential impact of contamination and imperfections on the surfaces. The thermal refractive power of the uncoated N-BK7 lens 9 is significantly larger than the thermal refractive power of the uncoated FS lenses 5 and 6. This indicates that the thermal refractive power of FS is significantly lower than the one of N-BK7.

As seen from Table 1, the coating has a much higher influence on the thermal refractive power than the substrate. The lowest thermal refractive powers were found for FS lenses with a WLC (lens no. 1, 2, and 3), but there are also large variations between the samples from the different manufacturers. This may be attributed to different coating materials and coating methods. BBC exhibit a more complex layer composition and therefore potentially lead to significantly larger thermal refractive power (lens no. 4).

Table 1. Experimentally determined thermal refractive power (column 7) and specifications (column 1-6) of the tested plano-convex lenses. The substrate of the lenses is either fused silica (FS) or N-BK7. The lenses are either uncoated (UC) or coated with a specific wavelength coating (WLC) or a broadband coating (BBC).

Number	Substrate	Coating type	Condition	Company	Focal length / mm	D* / 10^{-6} mm/W
1	FS	WLC	New	1	300	0.55
2	FS	WLC	Used	2	400	0.77
3	FS	WLC	Used	3	300	2.77
4	FS	BBC	New	4	250	6.51
5	FS	UC	Used	5	240	1.16
6	FS	UC	Used	5	500	1.27
7	N-BK7	WLC	New	4	250	1.93
8	N-BK7	BBC	New	6	250	20.43
9	N-BK7	UC	New	6	250	1.52

4. Thermally induced focal shift of thin lenses

With the known values of the intensity-specific thermal refractive powers of the various lenses discussed above Eq. (6) can be used to calculated the power-dependent focal shift. Assuming a beam propagation factor of M^2 = 1.2, the focal shift caused by FS and the N-BK7

Optics EXPRESS

lenses is shown in Fig. 3(a) and Fig. 3(b), respectively. The type of coating as well as the condition of the lens are listed in the corresponding legend. As a convenient criterion to assess the power handling capability of a lens one may define that the thermally induced focal shift should not exceed one Rayleigh length, as indicated by the horizontal dashed lines in Fig. 3. It can be seen clearly that on this condition all lenses made of N-BK7 are not suitable to endure an average laser power of 1 kW. Depending on the coating there are also lenses made of FS which lead to a thermally induced focal shift of more than one Rayleigh length per kW average laser power. But with a good WLC the FS lenses as well as uncoated and clean FS lenses lead to a thermal induced focal shift which is smaller than one Rayleigh length per kW of transmitted average laser power. The lowest thermally induced focal shift per kW average laser power (0.45 z_R per kW) was observed for a new (previously unused) lens made of FS with a WLC (lens 1).

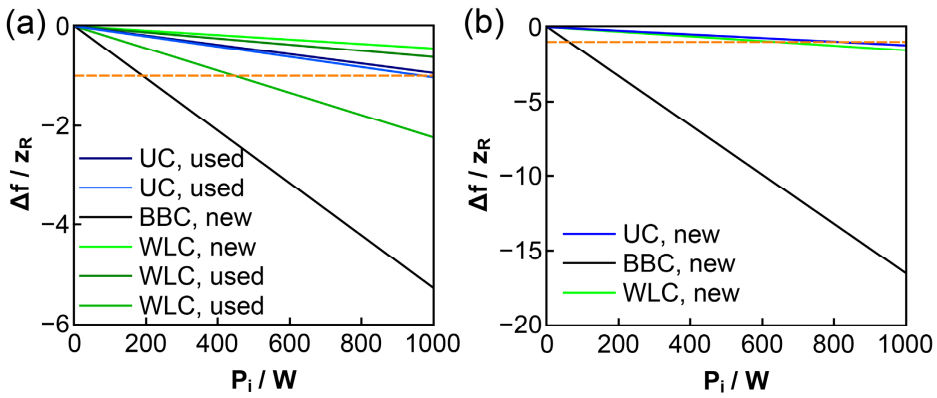

Fig. 3. Extrapolation of the thermally induced focal shift of thin lenses made of fused silica (a) and N-BK7 (b) with different coating types to average laser powers of up to 1000 W. The calculations are based on the experimentally determined thermal dioptric powers of the various lenses. The orange dashed line illustrates a focal shift of one Rayleigh-length z_R. Laser parameters: λ = 1030 nm, w_{cb} = 2.5 mm, M^2 = 1.2.

5. Conclusion

The thermal refractive power of thin lenses that are commonly used to focus the beam of ultrafast lasers for micro materials processing was determined and compared. The comparison reveals the influence of different substrates (fused silica and N-BK7) and coatings (uncoated, broadband coating, specific wavelength coating). Lenses made of fused silica generally cause a thermally induced focal shift which is about half the one observed with lenses made of N-BK7, but the coating type has an even more significant influence than the sole lens material. A specific wavelength coating of good quality causes no significant additional focal shift. A broadband coating was found to cause a significant additional thermally induced focal shift. The lenses made of N-BK7 were found to not be suitable for powers in the kW range, as the thermally induced focal shift significantly exceed one Rayleigh length. At 1 kW of transmitted power the focal shift thermally induced by lenses made of fused silica where found to be limited below one Rayleigh length only when they are either uncoated (and clean) or when they are coated with a specific wavelength coating of high quality.

The research will now be extended to further optics including F-Theta-objectives for static beams and small beam displacements on the lens that can still be measured with the presented setup and will be reported on at a later date.

Optics EXPRESS

6. Appendix

6.1 Thermally induced effects in the measurement setup

In order to take into account the thermally induced lens in the NDF in front of the CCD camera, we express the beam propagation starting at the focusing lens all the way through the measurement setup (Fig. 1) by means of the ABCD ray transfer matrix [17]

$$M = \begin{pmatrix} A & B \\ C & D \end{pmatrix} = \begin{pmatrix} 1 & 0 \\ -\frac{1}{f_{th,NDF}} & 1 \end{pmatrix} \cdot \begin{pmatrix} 1 & d \\ 0 & 1 \end{pmatrix} \cdot \begin{pmatrix} 1 & 0 \\ -\frac{1}{f_{th}} & 1 \end{pmatrix} \cdot \begin{pmatrix} 1 & 0 \\ -\frac{1}{f_0} & 1 \end{pmatrix}$$
$$= \begin{pmatrix} 1-\frac{d}{f_{th}}-\frac{d}{f_0} & d \\ -\frac{1}{f_0}-\frac{1}{f_{th}}-\frac{1}{f_{th,NDF}}+\frac{d}{f_0 \cdot f_{th,NDF}}+\frac{d}{f_{th} \cdot f_{th,NDF}} & 1-\frac{d}{f_{th,NDF}} \end{pmatrix}, \quad (9)$$

where d is the distance between the lens and the NDF, and $f_{th,NDF}$ is the thermally induced lens of the NDF. The NDF only contributes by its thermally induced dioptric power as its surfaces are flat. The refractive power of the complete system corresponds to element C of the matrix defined by Eq. (9) [18]. Using Eq. (1) this yields

$$\frac{1}{f_{tot}} = \frac{1 + f_0 \cdot D^* \cdot I_i + f_0 \cdot D^*_{NDF} \cdot I_{NDF} - d \cdot D^*_{NDF} \cdot I_{NDF} - d \cdot f_0 \cdot D^* \cdot I_i \cdot D^*_{NDF} \cdot I_{NDF}}{f_0}, \quad (10)$$

where D^*_{NDF} is intensity-specific the thermal refractive power of the NDF, and $I_{NDF} = R \cdot I_i / (1 - d / f_0)$ is the intensity incident on the NDF where R is the reflectivity of the beam splitter. To assess the influence of the thermally induced lens it is convenient to relate the thermally induced focal shift $\Delta f_{tot} = f_{tot} - f_0$ to the Rayleigh length z_R. The thermally induced focal shift caused by two optical elements in units of the Rayleigh length z_R is therefore now given by

$$\frac{\Delta f_{tot}}{z_R} = -\frac{f_0^2 \cdot D^* \cdot I_i + f_0^2 \cdot D^*_{NDF} \cdot \frac{R \cdot I_i}{1 - d/f_0} - d \cdot f_0 \cdot D^*_{NDF} \cdot \frac{R \cdot I_i}{1 - d/f_0} - d \cdot f_0^2 \cdot D^* \cdot I_i \cdot D^*_{NDF} \cdot \frac{R \cdot I_i}{1 - d/f_0}}{z_R \cdot \left(1 + f_0 \cdot D^* \cdot I_i + f_0 \cdot D^*_{NDF} \cdot \frac{R \cdot I_i}{1 - d/f_0} - d \cdot D^*_{NDF} \cdot \frac{R \cdot I_i}{1 - d/f_0} - d \cdot f_0 \cdot D^* \cdot I_i \cdot D^*_{NDF} \cdot \frac{R \cdot I_i}{1 - d/f_0}\right)}. \quad (11)$$

According to the asksumption $1/f_{th} \ll 1/f_0$ used above, Eq. (11) can also be approximated to read

$$\frac{\Delta f_{tot}}{z_R} \cong -\frac{f_0^2 \cdot D^* \cdot I_i + f_0^2 \cdot D^*_{NDF} \cdot \frac{R \cdot I_i}{1 - d/f_0} - d \cdot f_0 \cdot D^*_{NDF} \cdot \frac{R \cdot I_i}{1 - d/f_0} - d \cdot f_0^2 \cdot D^* \cdot I_i \cdot D^*_{NDF} \cdot \frac{R \cdot I_i}{1 - d/f_0}}{z_R \cdot \left(1 + f_0 \cdot D^*_{NDF} \cdot \frac{R \cdot I_i}{1 - d/f_0} - d \cdot D^*_{NDF} \cdot \frac{R \cdot I_i}{1 - d/f_0}\right)}. \quad (12)$$

As seen from the result, the value D^*_{NDF} needs to be known, in order to extract the thermal dioptric power D^* of the tested lens by a fit of the measured focal shift Δf with varying incident laser intensity I_i.

Optics EXPRESS

6.2 Determination of the thermal refractive power of the NDF

6.2.1 Experimental setup

To determine the thermal refractive power of the NDF the experimental setup shown in Fig. 4 was used. Only 0.72% of the laser beam power is reflected on the wedge towards the camera whereby the rest is guided to a water-cooled beam dump. The reflected beam was focused by lens 1 (FS, WLC, f = 300 mm). The maximum average laser power incident on this focusing lens was 4 W, on which condition the thermally induced focal shift in the focusing optics can be assumed to be negligible. According to Eq. (2) the thermally induced focal shift is a function of the intensity incident on the tested optics. To apply different intensities incident on the NDF for the same applied average laser powers, the NDF was positioned at different locations at 40 mm, 65 mm, 80 mm, 100 mm after the lens and directly in front of the lens. Since the focal length of the lens is much larger than the applied distances between the lens and the NDF, the beam radius onto the NDF can be calculated by ABCD-formalism. The beam radius of the collimated beam incident on the wedge was w_{cb} = 2.5 mm.

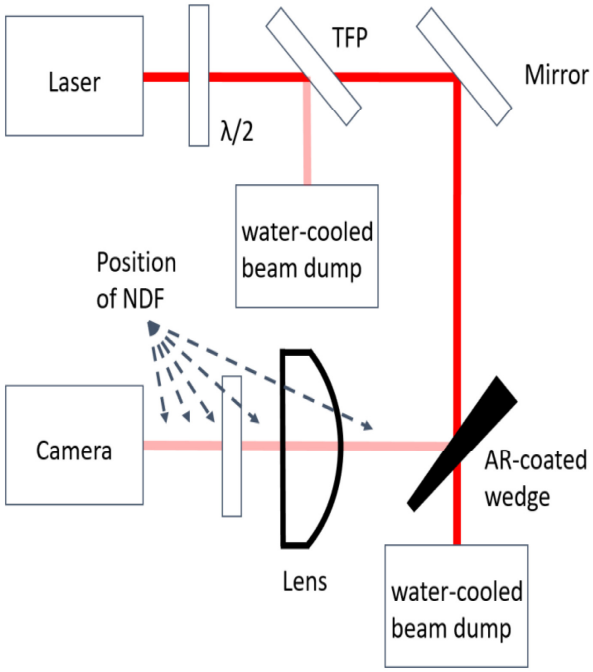

Fig. 4. Experimental setup for the measurement of the thermally induced focal shift of the NDF. A neutral-density filter (NDF) attenuates the beam reflected by the AR-coated wedge to avoid damages of the CCD chip of the camera.

6.2.2 Experimental results

Since the NDF is the only optics contributing to the measured focal shift Eq. (2) can be used to determine the thermal refractive power of the NDF. Since the reference with I_i = 0 and Δf_{NDF} = 0 is usually not well defined in the experiment, the determination of Δf_{NDF} as a function of the applied intensity I_i was first measured with respect to an arbitrary reference with an initially unknown offset Δf_0. Eq. (2) therefore is changed to

$$\frac{\Delta f_{NDF}}{z_R} = -\frac{f_0^2 \cdot D^*_{NDF} \cdot I_i}{z_R \cdot \left(1 + f_0 \cdot D^*_{NDF} \cdot I_i\right)} + \Delta f_0 . \tag{13}$$

Optics EXPRESS

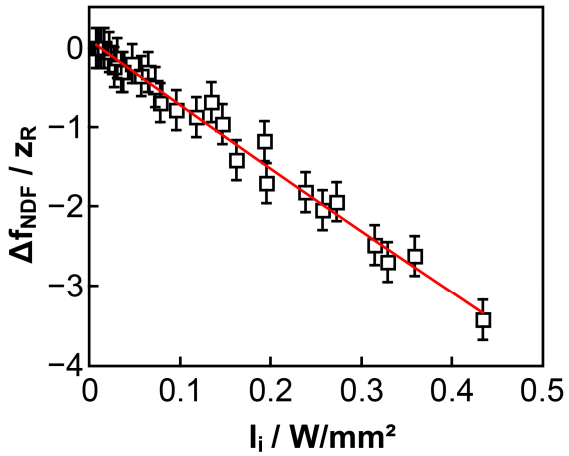

Fig. 5. Measured thermally induced focal shift caused by the NDF as a function of the incident average intensity (square data points). The red curve is a fit of Eq. (13) to the measured data. Laser parameters: λ = 1030 nm, w_{cb} = 2.5 mm, M^2 = 1.2, f = 300 kHz.

Figure 5 shows the measured thermally induced focal shift (in units of the Rayleigh length of the probe beam) caused by the NDF. The Rayleigh length of the focused laser beam was determined to be z_R = 3.62 mm. By fitting Eq. (2) to the measured data (least square fit with D^*_{NDF} and Δf_0 as the fitting parameters) shown in Fig 5, the thermal refractive power of the NDF was found to be

$$D^*_{NDF} = 3.32 \cdot 10^{-4} \frac{\text{mm}}{\text{W}} \tag{14}$$

Since the measured data agree very well with theory the above determination of the thermal refractive powers of thin lenses is reliable.

Funding

German Federal Ministry of Education and Research (grant number 13N13931).

References

1. D. B. Leviton and B. J. Frey, "Temperature-dependent absolute refractive index measurements of synthetic fused silica," in, SPIE Proceedings (SPIE, 2006), 62732K.
2. P.-E. Dupouy, M. Büchner, P. Paquier, G. Trénec, and J. Vigué, "Interferometric measurement of the temperature dependence of an index of refraction: application to fused silica," Appl. Opt. **49**(4), 678–682 (2010).
3. R. Weber, B. Neuenschwander, and H. P. Weber, "Thermal effects in solid-state laser materials," Opt. Mater. **11**(2-3), 245–254 (1999).
4. A. Forbes, *Laser Beam Propagation. Generation and Propagation of Customized Light* (Taylor and Francis, 2014).
5. B. Jaeggi, B. Neuenschwander, M. Schmid, M. Muralt, J. Zuercher, and U. Hunziker, "Influence of the Pulse Duration in the ps-Regime on the Ablation Efficiency of Metals," Phys. Procedia **12**, 164–171 (2011).
6. B. Wu, M. Zhou, J. Li, X. Ye, G. Li, and L. Cai, "Superhydrophobic surfaces fabricated by microstructuring of stainless steel using a femtosecond laser," Appl. Surf. Sci. **256**(1), 61–66 (2009).
7. R. Weber, T. Graf, P. Berger, V. Onuseit, M. Wiedenmann, C. Freitag, and A. Feuer, "Heat accumulation during pulsed laser materials processing," Opt. Express **22**(9), 11312–11324 (2014).
8. R. Weber, T. Graf, C. Freitag, A. Feuer, T. Kononenko, and V. I. Konov, "Processing constraints resulting from heat accumulation during pulsed and repetitive laser materials processing," Opt. Express **25**(4), 3966–3979 (2017).
9. S. Faas, U. Bielke, R. Weber, and T. Graf, "Prediction of the surface structures resulting from heat accumulation during processing with picosecond laser pulses at the average power of 420 W," Appl. Phys., A Mater. Sci. Process. **124**(9), 612 (2018).

Optics EXPRESS

10. C. Thiel, R. Weber, J. Johannsen, and T. Graf, "Stabilization of a Laser Welding Process Against Focal Shift Effects using Beam Manipulation," Phys. Procedia **41**, 209–215 (2013).
11. C. Freitag, M. Wiedenmann, J.-P. Negel, A. Loescher, V. Onuseit, R. Weber, M. Abdou Ahmed, and T. Graf, "High-quality processing of CFRP with a 1.1-kW picosecond laser," Appl. Phys., A Mater. Sci. Process. **119**(4), 1237–1243 (2015).
12. J.-P. Negel, A. Voss, M. Abdou Ahmed, D. Bauer, D. Sutter, A. Killi, and T. Graf, "1.1 kW average output power from a thin-disk multipass amplifier for ultrashort laser pulses," Opt. Lett. **38**(24), 5442–5445 (2013).
13. J.-P. Negel, A. Loescher, D. Bauer, D. Sutter, A. Killi, M. Abdou Ahmed, and T. Graf, "Second Generation Thin-Disk Multipass Amplifier Delivering Picosecond Pulses with 2 kW of Average Output Power," in *Applications of Lasers for Sensing and Free Space Communications. Part of Lasers: 30 October-3 November 2016, Boston, Massachusetts, United States*, OSA technical digest (online) (OSA - The Optical Society, 2016), ATu4A.5.
14. T. Graf, J. E. Balmer, R. Weber, and H. P. Weber, "Multi-Nd. YAG-rod variable-configuration resonator (VCR) end pumped by multiple diode-laser bars," Opt. Commun. **135**(1-3), 171–178 (1997).
15. W. Koechner, *Solid-State Laser Engineering* (Springer, 2006).
16. T. Graf, *Laser. Grundlagen der Laserstrahlerzeugung*, 2., überarbeitete und erweiterte Auflage (Springer Vieweg, 2015).
17. H. Hügel and T. Graf, *Laser in der Fertigung. Strahlquellen, Systeme, Fertigungsverfahren*, 3., überarb. und erw. Aufl. (Springer Fachmedien Wiesbaden GmbH, 2014).
18. B. E. A. Saleh, M. C. Teich, and J. W. Goodman, *Fundamentals of Photonics* (John Wiley & Sons, Inc, 1991).